Supplementary Information

Polystyrene diameter calculation:

The diameter of the PS was calculated for different plasma-treated samples (T_p = 0 to 240 s) using ImageJ software. The statistical distribution of the diameter plotted in Figs. S1a-e shows that the count of lower diameter increases with an increase in T_p. Fig S1f shows that the average diameter of the PS spheres decreases with an increase in OPT time. The etching of PS is caused by the reaction of the carbon of PS with the oxygen to form CO2, CO, etc. gases.[1]

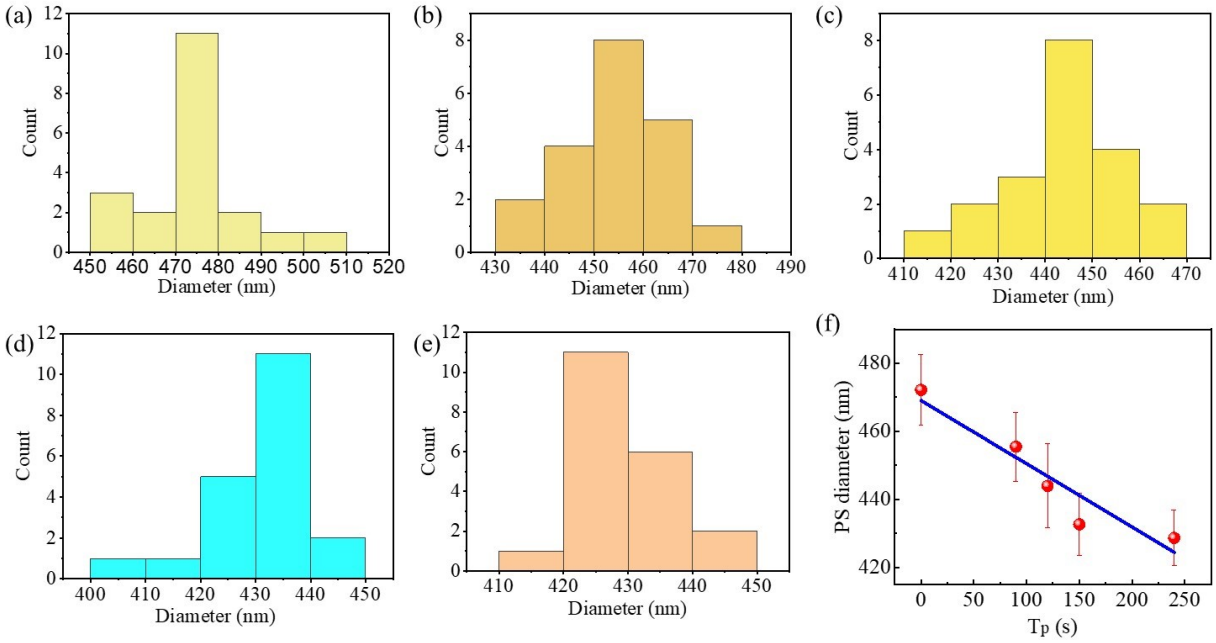

Fig. S1 Statistical distribution of diameter of the PS nanospheres with T_p = (a) 0, (b) 90, (c), 120, (d) 150, and (e) 240 s. (f) PS sphere diameter as a function of plasma treatment time (T_p).

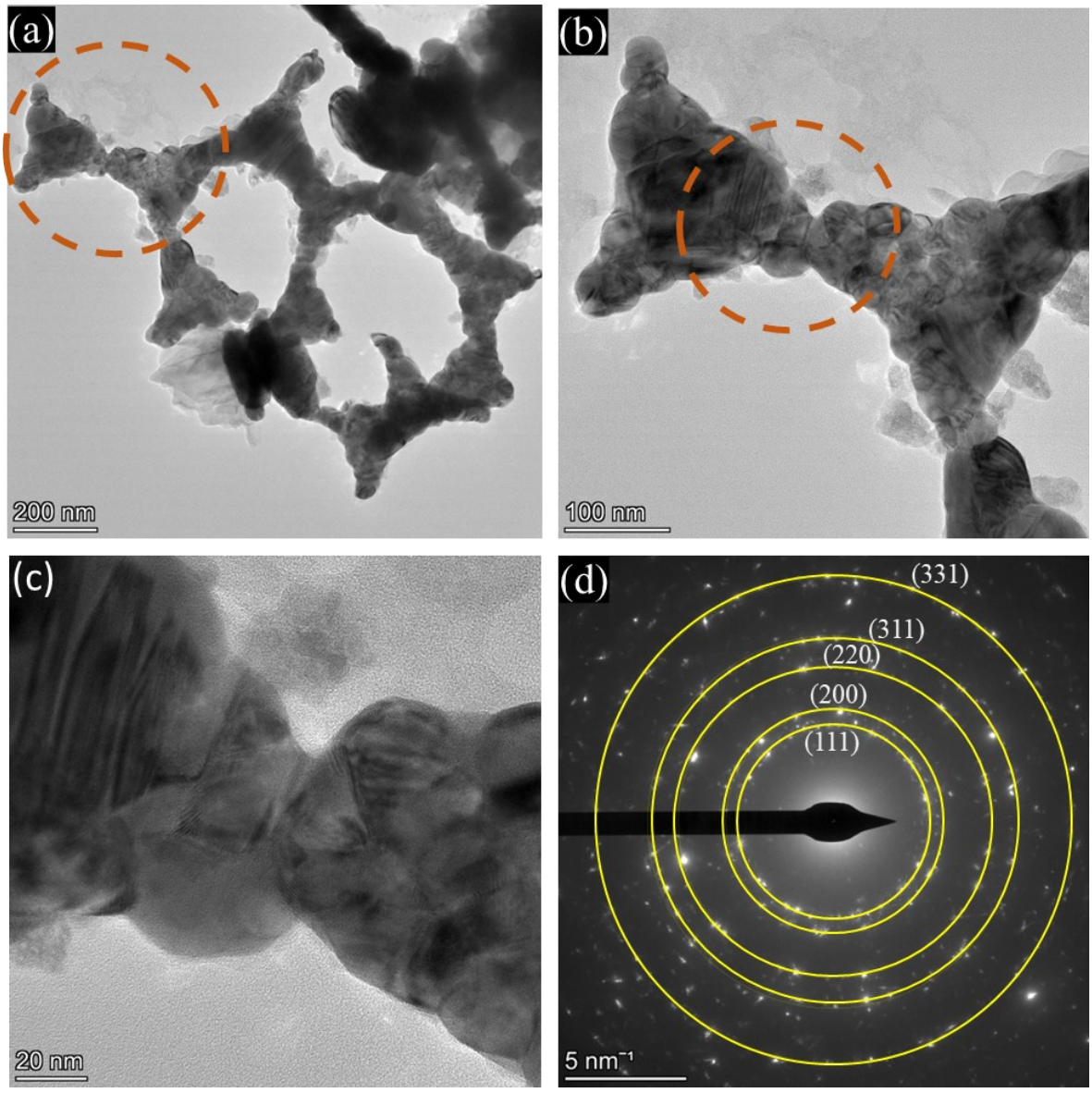

Fig. S2 (a) Bright-field TEM image of Ag triangular structure. (b) and (c) are the magnified images of the dashed circular region in (a) and (b), respectively. (d) SAED pattern.

Table S1. Calculation of planes corresponding to SAED pattern.

1/2r	1/r	r (nm)	$d_{calculated}$ (Å)	(hkl)
8.184	4.092	0.249	2.49	(111)
9.127	4.5635	0.219	2.19	(200)
12.950	6.475	0.154	1.54	(220)
15.246	7.623	0.131	1.31	(311)
20.86	10.43	0.095	0.95	(331)

Fill factor and nanogap calculation:

The fill factor and average nanogap were calculated using ImageJ software, as shown in Fig. S3. All the nanogaps were calculated and divided by the total number of nanogap to get the average nanogap. The calculated fill factor and average nanogap are indexed in Table S2.

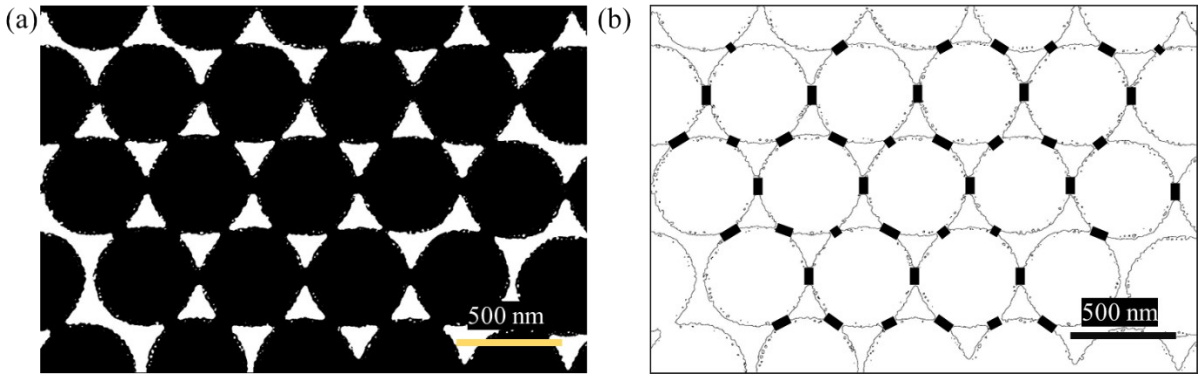

Fig. S3 (a) Fill factor and (b) average nanogap of triangular nanostructure calculation using ImageJ software.

Table S2

Parameters	T_p = 0 s	T_p = 90 s	T_p = 120 s	T_p = 150 s	T_p = 240 s
Fill factor	11.08 %	15.2 %	17.5 %	19.83 %	24. 89 %
Average Nanogap	104 nm	78 nm	64 nm	54 nm	15 nm

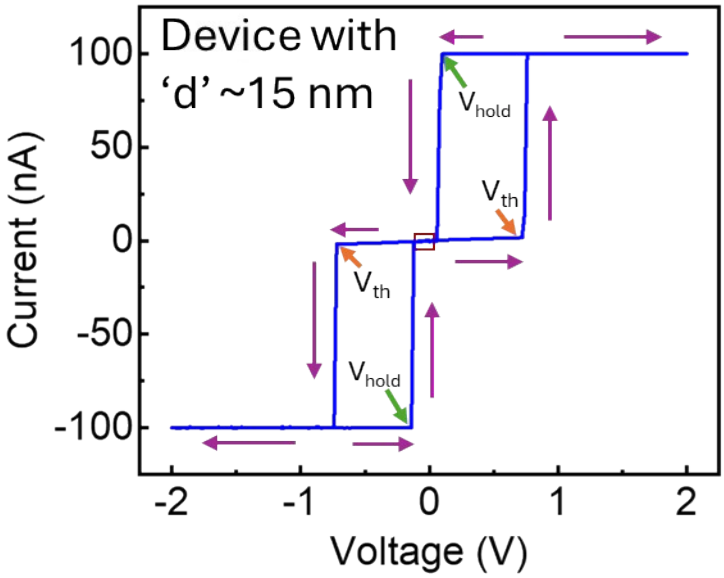

Fig. S4 I-V sweep of the device ('d' ~ 15 nm) in both the positive and negative voltage. The red box around the origin shows the voltage window for erasing LRS. Orange arrows indicate the threshold switching (V_{th}), and green arrows denote the holding voltage (V_{hold}). Violet arrows are for the direction of the sweep.

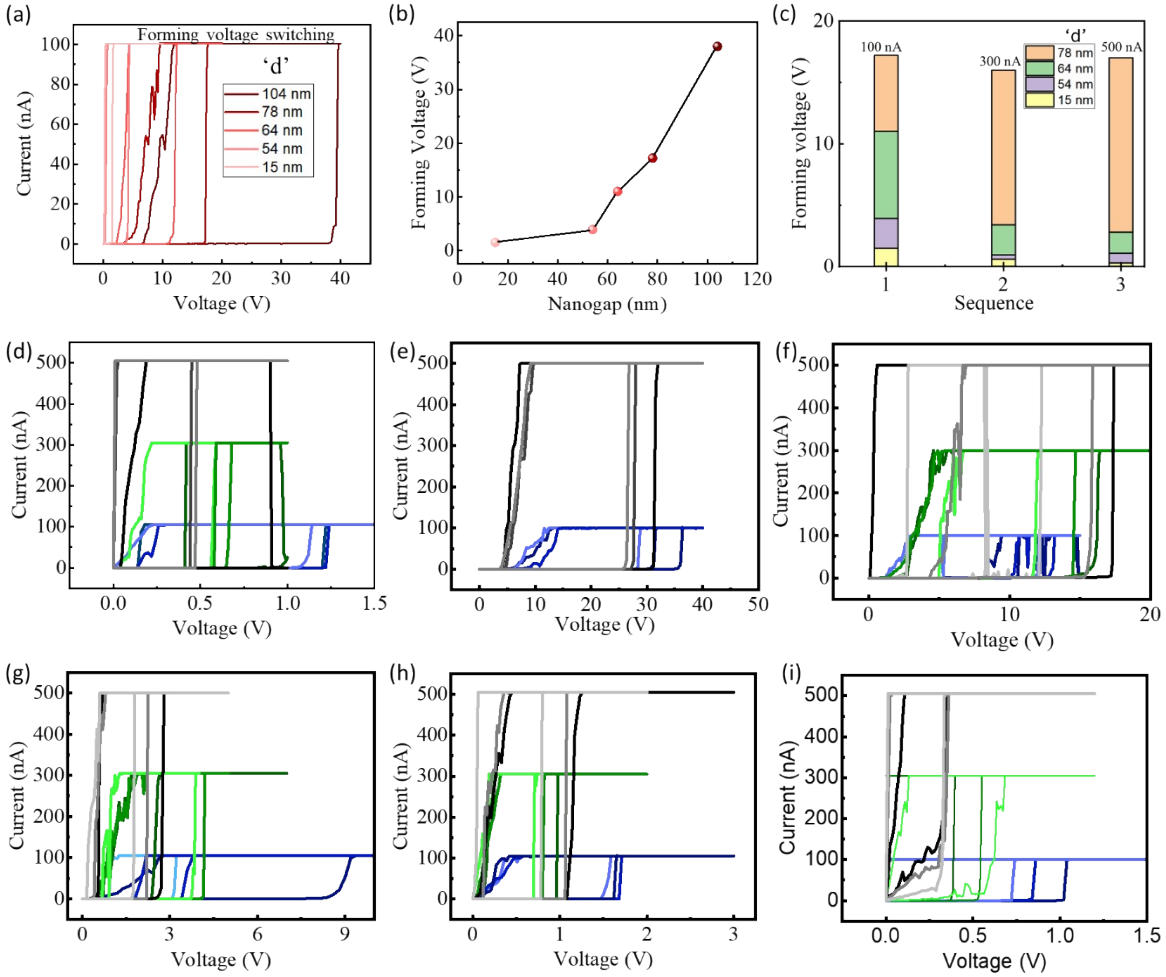

Fig. S5 (a) Forming voltage switching of the device at each nanogap 'd' (b) Forming voltage variation with nanogap and (c) histogram of forming voltage vs sequence of sweep for each nanogap (~ d) device. Repetitive I-V sweeps of devices having (d) QT structure, (e) d ~ 104 nm, (f) d ~ 78 nm, (g) d ~ 64 nm, (h) d ~ 54 nm, and (i) d ~ 15 nm at current compliance of 100, 300 and 500 nA. Note: The device with d ~ 104 nm has not been added to the histogram because of the high threshold switching and the color gradient of plots represents consecutive sweeps.

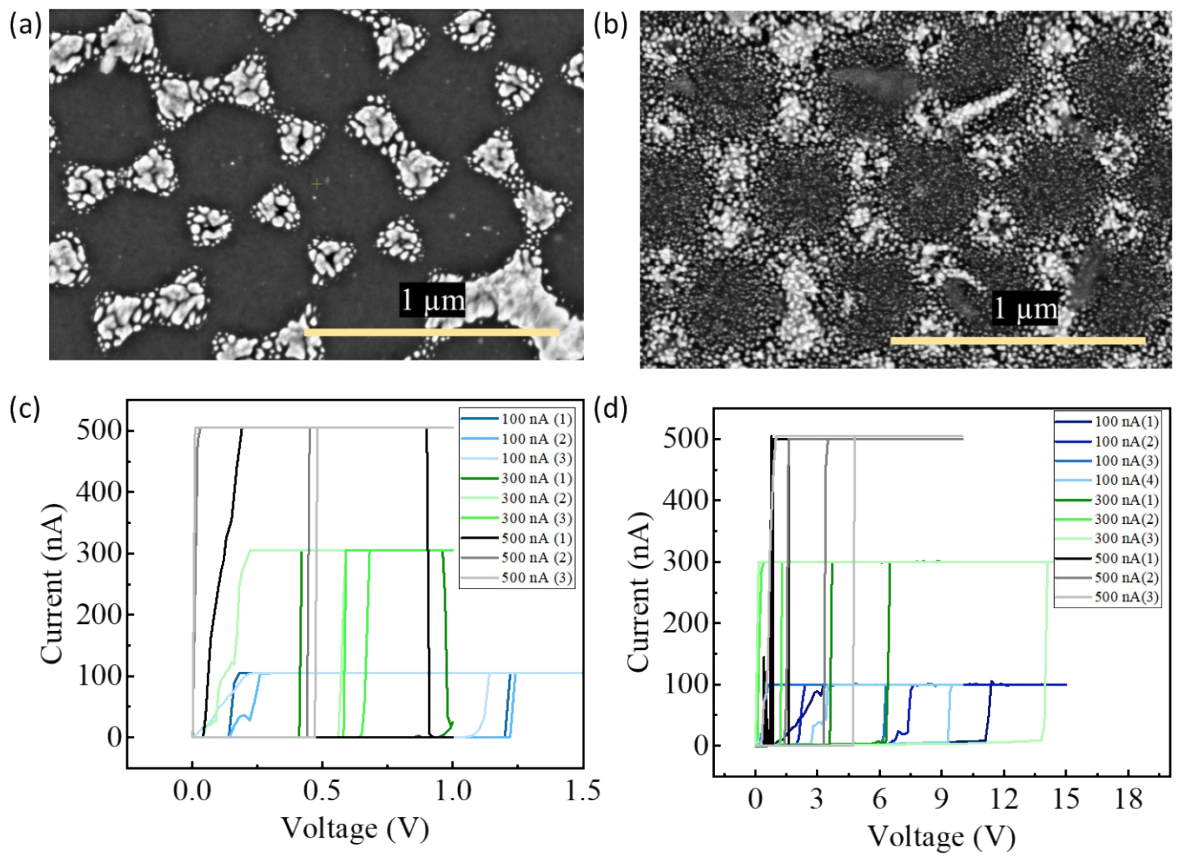

Fig. S6 (a) and (b) SEM images before and after the electrical pulsing, respectively, for the device with QT structure. I-V sweeps (c) before and (d) after pulsing, there was an order of increment in V_{th} post-pulsing, indicating instability of the device.

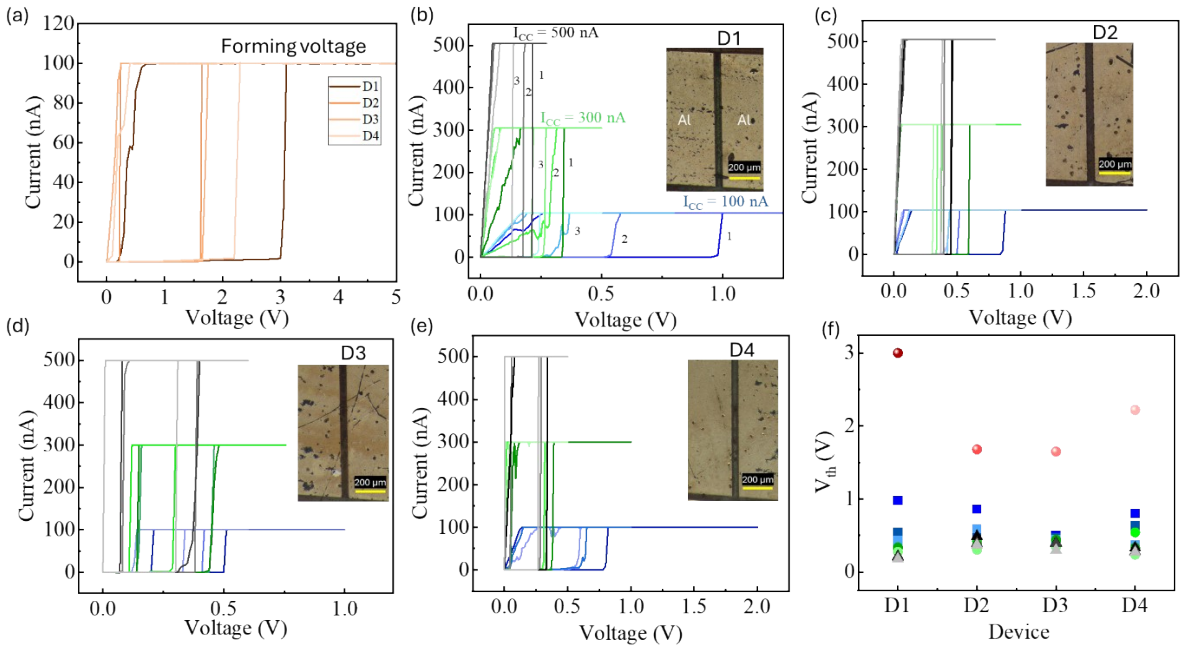

Fig. S7 Device-to-device variability of devices D1, D2, D3, and D4 with nanogap of 'd' ~ 15 nm. (a) I-V sweeps showing the forming voltage of these devices. The successive I-V sweeps of four devices (b) D1, (c) D2, (d) D3, and (e) D4 at I_{CC} of 100, 300, and 500 nA. Insets showing

optical microscopy images of the devices. (f) Variation in forming and threshold voltage across all devices. Brown curves and points denote forming voltage, while blue, green, and black curves and points correspond to a threshold voltage at 100 nA, 300 nA, and 500 nA.

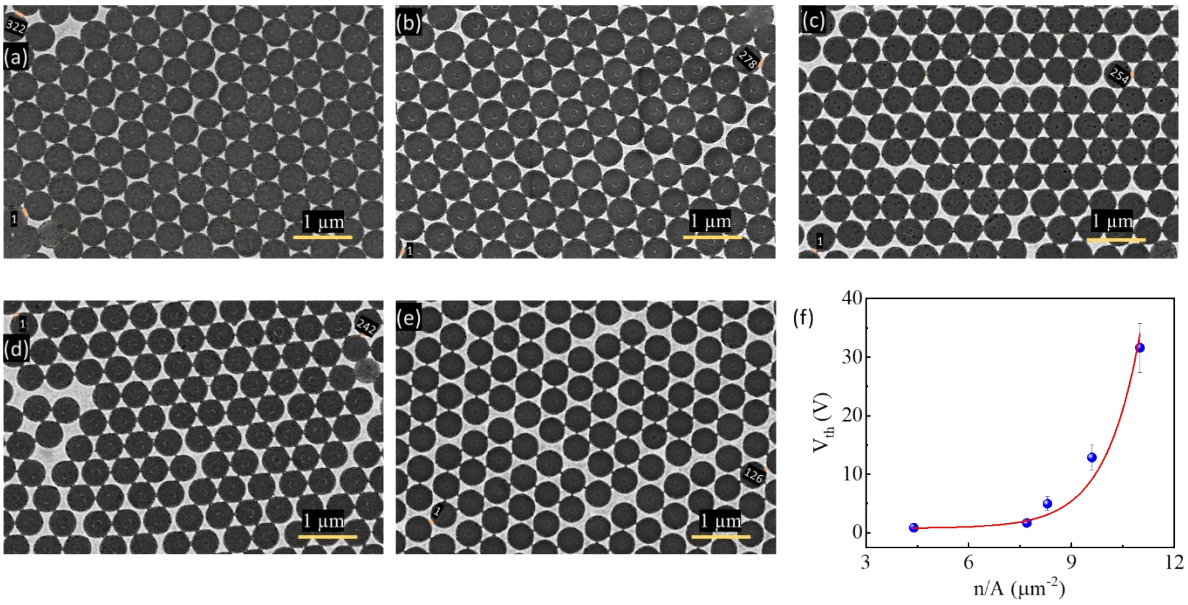

Fig. S8 Number density and average nanogap calculation for the samples with (a) 0, (b) 90, (c) 120, (d) 150, (e) 240 s T_p using ImageJ software, and (f) threshold voltage variation with the number density of nanogap. n and A are the number of nanogaps and the area of the image.

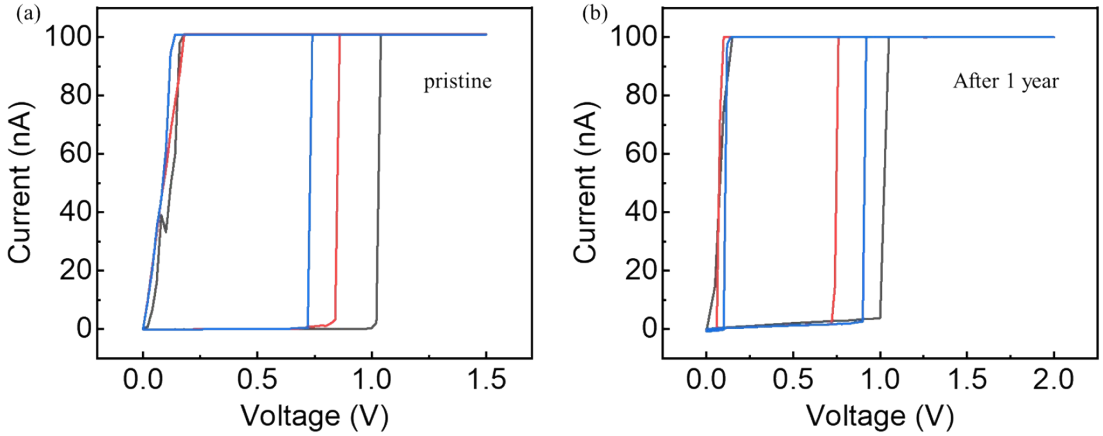

Fig. S9 I-V sweep of the pristine device ('d' ~15 nm) and the same device after one year.

Energy consumption calculation:

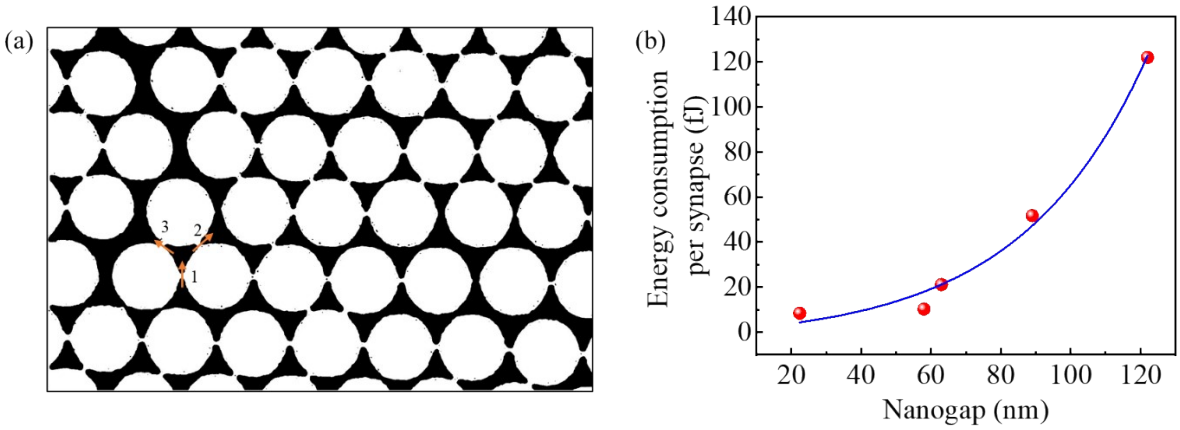

Fig. S10 (a) FESEM binary image of the Ag triangles of d = 15 nm nanogap device, illustrating that each triangle has two probable paths for synaptic connection formation, indicated by arrows 2 and 3. (b) Plot of the energy consumption per synapse of the device with nanogap.

Note S1

Energy consumed for the electromigration of the Ag ions to form the junction between the nanotriangles can be calculated by the formula[2]:

$$E_0 = V_{th} \times I_{CC} \times t_w \qquad \text{(S1)}$$

$$= 0.86(V) \times 100(nA) \times 50(ms) = 4.3 \text{ nJ (for device with d = 15 nm nanogap)}$$

Taking the assumption that the number of the synaptic path for each nanotriangle, n=2

Area of binary image, $= 8.972\ \mu m^2 = 1.39 \times 10^{-8}\ (inch)^2$

Total number of Ag triangles in $8.972\ \mu m^2 = 29$

Ag triangles density, $\rho = 29/1.39 \times 10^{-8}\ (inch)^2 = 2.086 \times 10^9\ /(inch)^2$

Synaptic junction density, $N_0 = \rho \times n = 2.086 \times 10^9 \times 2 = 4.172 \times 10^9\ /(inch)^2$

Energy density, $E_s = E_0/A = 4.3/39.2 \times 2000 \times 39.37 \times 39.37 = 3.53 \times 10^4\ nJ/(inch)^2$

Energy consumed per unit synapse= $E_s/N_0 = 3.53 \times 10^{-5}/4.172 \times 10^9 = 8.4$ fJ

The energy consumption per synapse for all the samples with varied nanogaps was calculated using the equation S1. The only parameter V_{th} is changing in the calculation for different nanogaps. Higher nanogap devices consume more energy than lower ones, as shown in Fig. S10b.

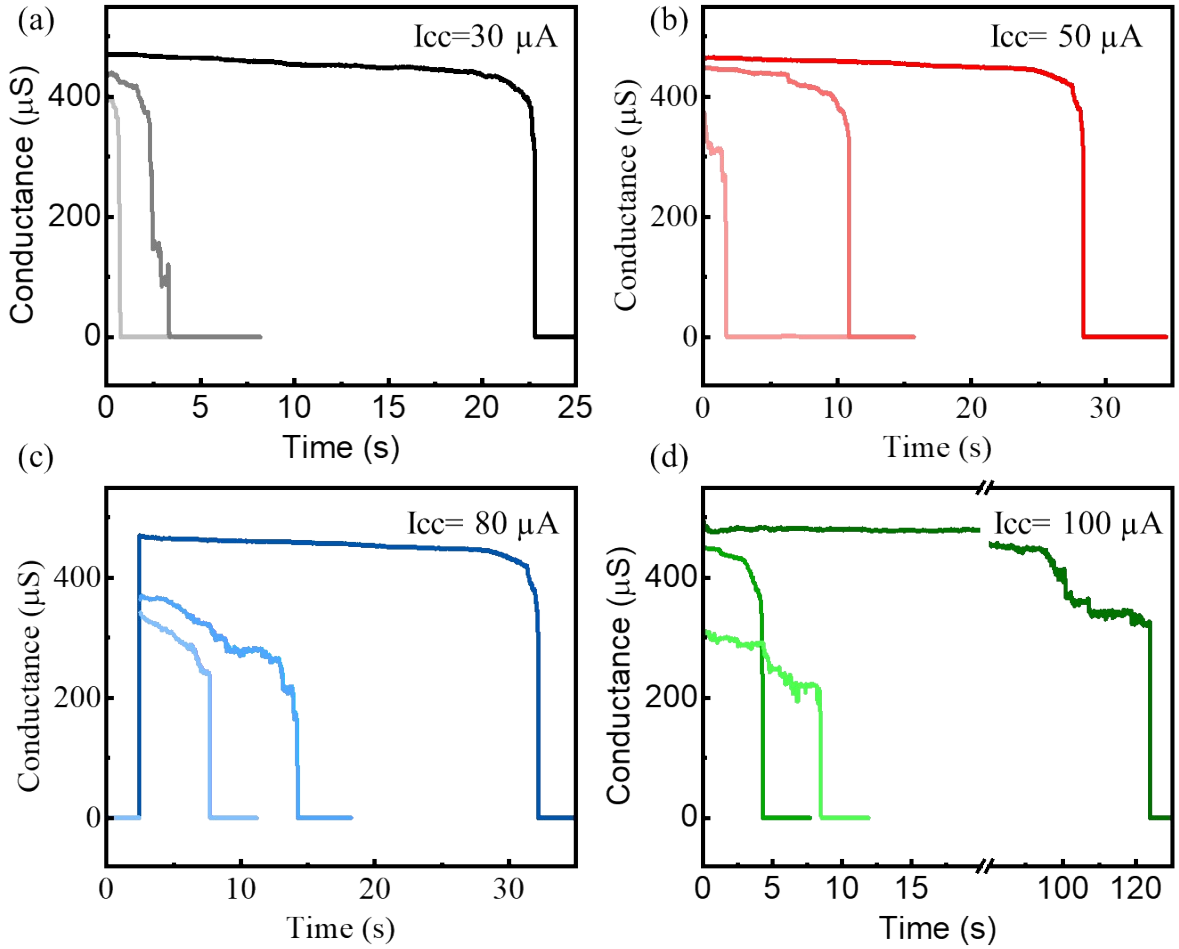

Fig. S11 Memory retention with three repetitive pulsing at compliance (a) 30, (b) 50, (c) 80, and (d) 100 µA for a device having QT structure.

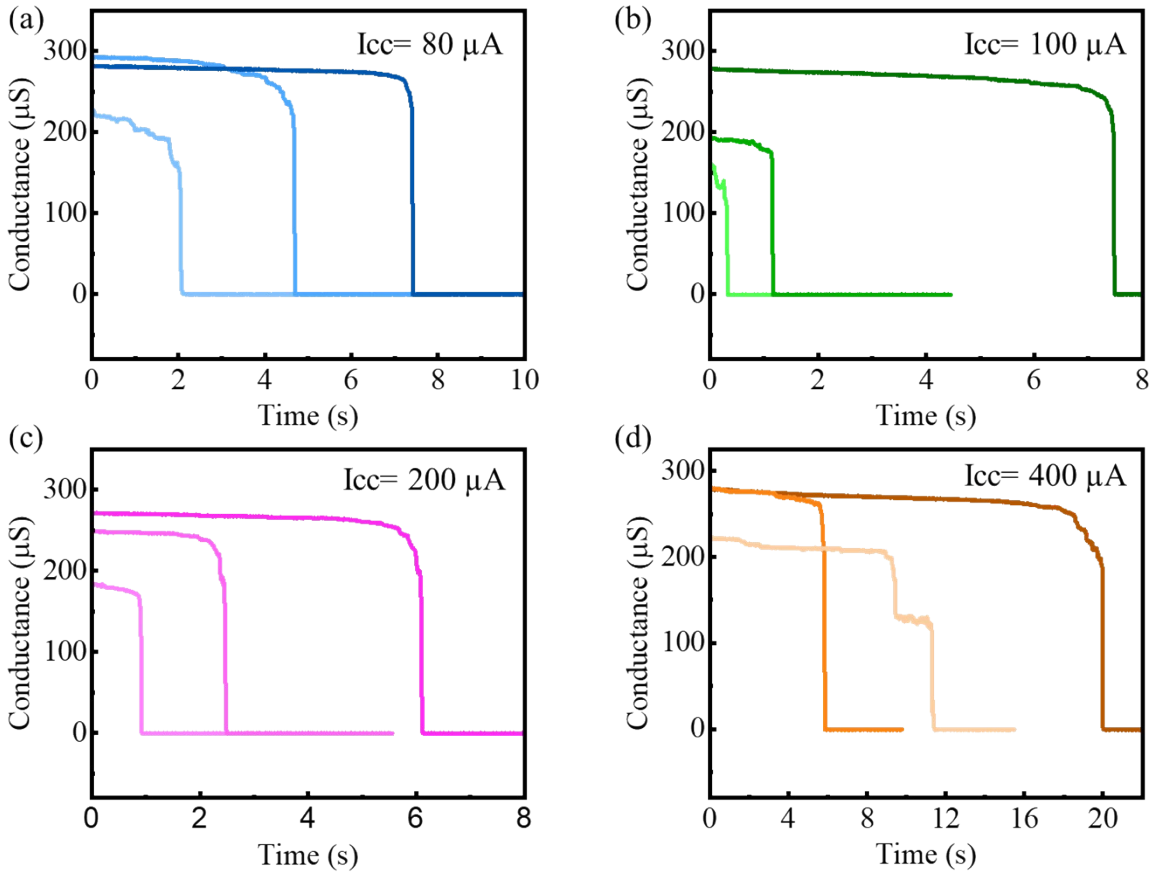

Fig. S12 Memory retention with three repetitive pulsing at each compliance (a) 80 (b) 100 (c) 200 (d) 400 µA for a device having nanogap d ~ 64 nm.

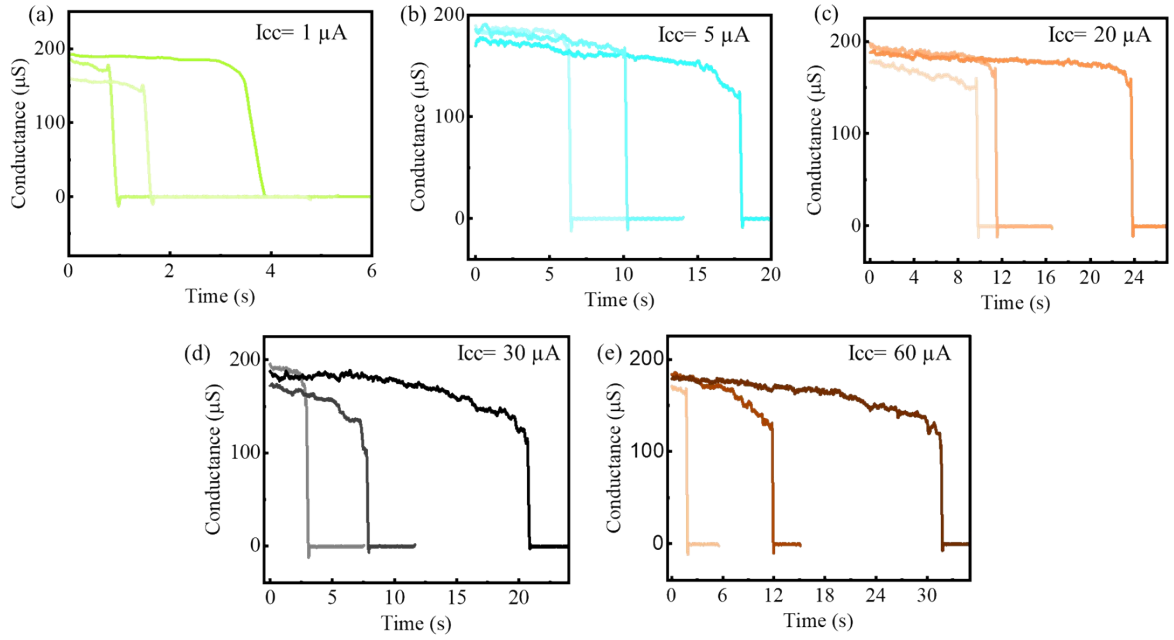

Fig S13 Memory retention with three repetitive pulsing at each compliance (a) 1, (b) 5, (c) 20, (d) 30, and (e) 60 µA for a device having nanogap d ~ 54 nm.

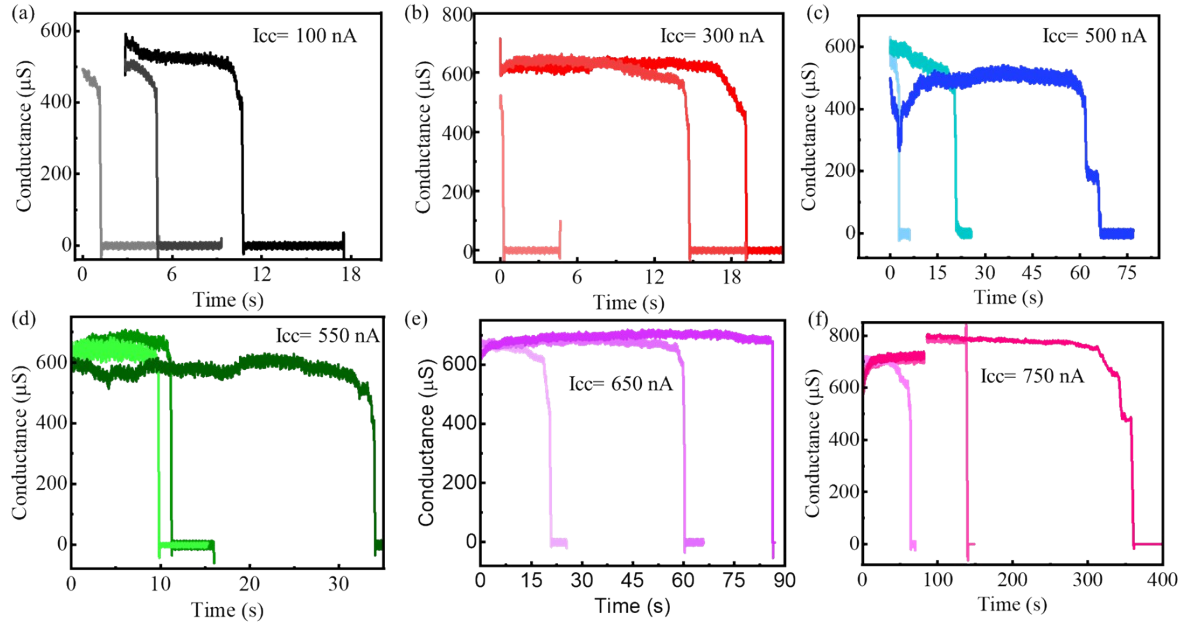

Fig S14 Memory retention with three repetitive pulsing at each compliance (a) 100, (b) 300, (c) 500, (d) 550, (e) 650, and (f) 750 nA for a device having nanogap d ~ 15 nm.

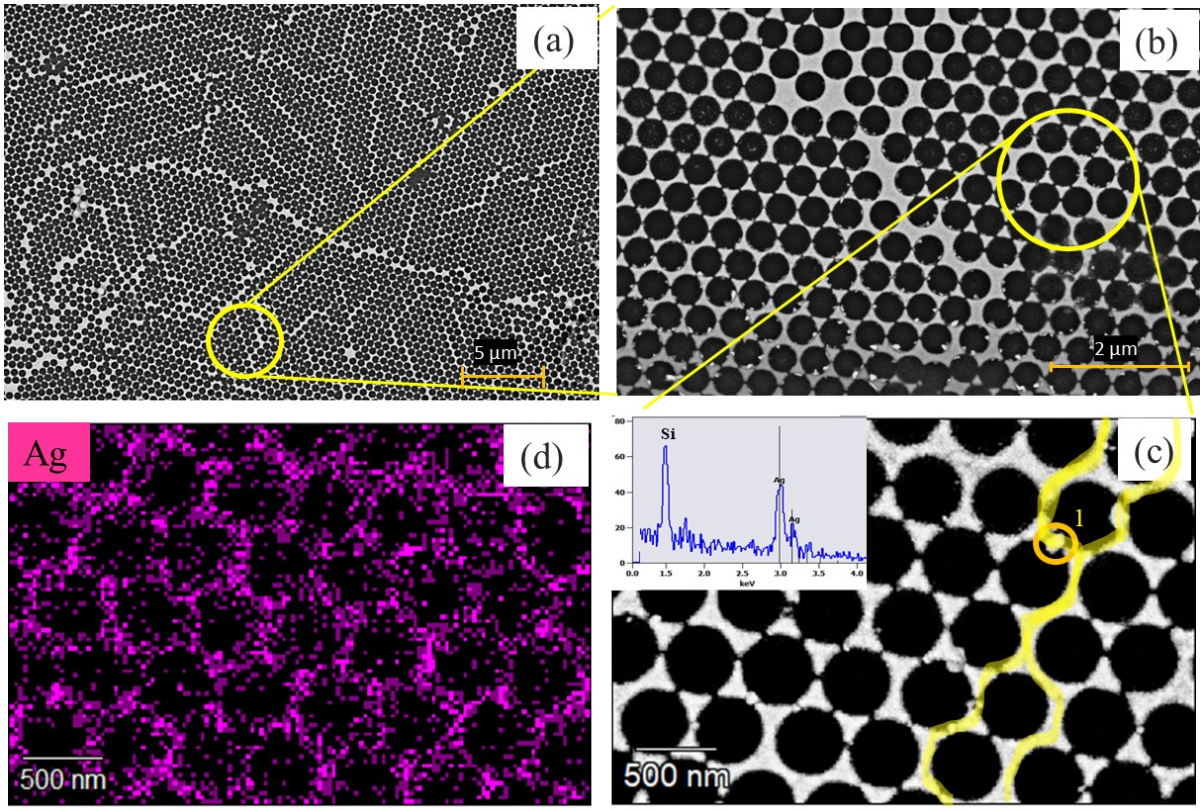

Fig S15 (a) SEM image of Ag nanostructures after pulsing. (b) and (c) Magnified images of the marked region; inset: EDS spectrum of the marked point in (c), and (d) elemental mapping of (c).

Note S2

COMSOL Multiphysics simulation details:

The electric field distribution of the Ag bowtie fabricated by NSL method is important for getting information about the probable filamentary path across the electrodes. COMSOL Multiphysics software calculates the electrical field distribution of intact and quasi-triangular periodic structures. FESEM binary image is converted into curve images for the simulation. According to the V_{th} of resistive switching (Fig 3), 0.5 V and 1 V were applied across the Al electrodes of intact triangular and QT structures, respectively. The gap between the electrodes is 5.12 µm and 2.08 µm in Fig 6d and 6e, respectively. The field distribution using the electrostatics physics is calculated by Poisson's equation:

$$\nabla \cdot E = \frac{\rho}{\varepsilon_0 \varepsilon_r}$$

Where, E= Electric field intensity, ρ= Charge density, ε_0 and ε_r are the relative permittivity and permittivity of vacuum. The ε_r values of aluminum[3] and silver[4] are taken from the COMSOL library. The maximum electric field intensity is localized between the lowest nanogap region. Figs 6d and 6e show that the maximum electric fields are 10^7 V/m and 8×10^6 V/m for the lowest nanogaps.

References:

1 A. A. Osipov, A. E. Gagaeva, A. B. Speshilova, E. V. Endiiarova, P. G. Bespalova, A. A. Osipov, I. A. Belyanov, K. S. Tyurikov, I. A. Tyurikova and S. E. Alexandrov, *Sci Rep*, 2023, **13**, 3350.

2 R. Attri, I. Mondal, B. Yadav, G. U. Kulkarni and C. N. R. Rao, *Mater Horiz*, 2023, **11**, 737–746.

3 A. D. R. Rakic´, *Applied optics*, 1995, **22**, 4755-4767.

4 D. Koelling, A. Freeman, F. Mueller, P. B. Johnson and R. W. Christy, *Phys Rev B*, 1963, **11**, 3093.